Density imaging of volcanos with atmospheric muons

F. Fehr

Density Imaging of Volcanos with Atmospheric Muons

FELIX FEHR[1], for the TOMUVOL Collaboration*

[1] *Laboratoire de Physique Corpusculaire, Clermont-Ferrand, *http://www.tomuvol.fr*

fehr@clermont.in2p3.fr

Abstract: Their capability to penetrate large depths of material renders high-energy atmospheric muons a unique probe for geophysical explorations. Provided the topography of the target is known, the measurement of the attenuation of the muon flux permits the cartography of matter density distributions revealing spatial and possibly also temporal variations in extended geological structures. A Collaboration between volcanologists, astroparticle- and particle physicists, TOMU-VOL, was formed in 2009 to study tomographic muon imaging of volcanos with high-resolution tracking detectors. This contribution presents preparatory work towards muon tomography as well as flux measurements obtained after the first months of data taking at the Puy de Dôme, an inactive lava dome volcano in the Massif Central in south-central France.

Keywords: Volcanos; Atmospheric Muons; Muon Imaging

1 Introduction

Cosmic rays impinging upon Earth interact with atoms in the atmosphere to produce a continuous flux of high-energy, secondary muons. Since these muons are, depending on their energy, able to penetrate large depths of material, they can serve as a unique probe for geophysical research.

The idea of using atmospheric muons for probing extended structures is itself not new. In fact, atmospheric muons were used to estimate the snow overburden on a mountain tunnel as early as 1955 [1] and the first archaeological prospection based on muon imaging dates back to the early 1960s, when L.W. Alvarez et al. were searching for hidden chambers in Chepren's pyramid [2].

Today, new particle detectors motivate further studies to exploit the full potential of muon imaging. One of the most exciting applications is the exploration of volcanos [3]; this is pursued by the TOMUVOL Collaboration. Initiated in 2009, TOMUVOL is a common project of particle- and astroparticle physicists and volcanologists who collaborate on the development of a robust, portable system for imaging of volcanos using atmospheric muons. Such a system can complement traditional methods (i.e. gravimetric and electrical resistivity measurements) to improve the understanding of volcanic structures and might also help to reduce volcanic hazards.

The basic idea behind muon imaging of volcanos is that measuring the absorption of the muon flux as function of the direction at a fixed location permits mapping out the average column density in the volcano once the topography is known. By repeating the measurement from different locations, three-dimensional models of the matter density distribution can then be computed. These models will be of great interest to volcanologists, as matter density can readily be interpreted in terms of state and transition.

Presently, the TOMUVOL Collaboration is operating a muon detector at the flank of the Puy de Dôme, an inactive volcanic dome in the *Chaîne des Puys* [4] situated in the Massif Central (south-central France). In the initial phase of the project, muon flux measurements were performed and the data are now analyzed to obtain a first radiographic image. The next phase is dedicated to taking a detailed three-dimensional map of the density distribution in the Puy de Dôme and to validate the results by comparing with gravimetric and electrical resistivity measurements on the same site. In the future, after technical enhancements, the same methodology might be applied to other targets.

In the present paper we report on preparatory work and measurements taken at the Puy de Dôme in the initial phase of the project. In Section 2, the detection site and the experimental setup are described in some detail. Important experimental aspects including detector positioning and track reconstruction are considered. Preliminary results of the first months of data taking are then presented in Section 3. Based on this, we evaluate the prospects of muon imaging in the concluding section.

2 The Experiment at the Puy de Dôme

Detection Site The Puy de Dôme (alt. 1464 m a.s.l.) is of volcanic origin and was formed some $11,000$ years ago [5]. It has a remarkable structure with two domes originating
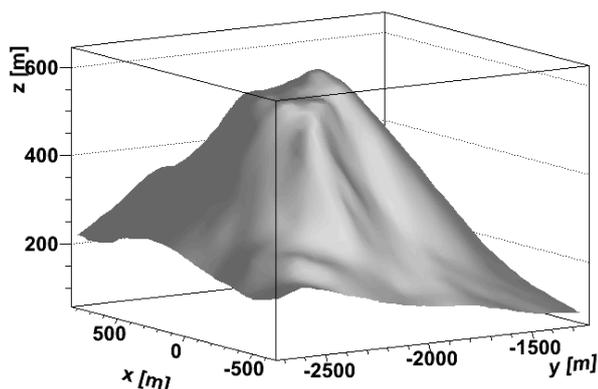
Figure 1: Topography of the Puy de Dôme. The origin indicates the position of the detector during the first months.

Figure 2: Acceptance of the initial setup ($\mathcal{A} = 0.16$ m^2) evaluated with a ray-tracing simulation.

from two subsequent eruptions, which occurred within a short time interval.

For the first radiographic measurements, a muon detector has been installed 600 m below the summit at a distance of 2 km. The detector has been deployed underground in a basement to reduce the impact of low-energy background. Figure 1 displays the location of the detector and the topography of the surrounding area.

Muon Detector and Data Taking Main requirements on the muon detector are good resolution, low noise, robustness, portability, and scalability at low cost. The TOMU-VOL Collaboration has opted for a muon detector based on three parallel planes of Glass Resistive Plate Chambers (GRPCs) [6]. A single chamber consists of two parallel thin glass plates kept at a distance of about 1 mm using tiny ceramic balls as spacers so that gas can circulate between the plates. The outer sides of the glass plates are coated with a thin layer of highly resistive material on which high voltage, typically 7 kV, is applied. A thin Mylar layer serves as insulation between the anode and a layer of copper cells of 1 cm^2 size assembled on one face of a Printed Circuit Board (PCB) of 50.0×33.3 cm^2. On the other face of the PCB are attached the readout ASICs, named HARDROC2 [7]. In total 48 HARDROC2 ASICs are connected on one PCB, each of them handling 8×8 pads. A full square meter chamber consists then of three slabs, each with two PCBs, having in total 9142 readout channels. The chambers are embedded in steel cassettes and are vertically mounted onto a movable aluminum support framework.

Charged particles, passing through the chambers, ionize the gas and produce charge cascades, which in turn induce charge signals on the copper plates. In its standard configuration, the detector is operated in avalanche mode with high voltage being adapted to environmental pressure and temperature conditions. The gas is a mixture of forane (93%), isobutane (5%) and SF6 (2%) regulated to a total throughput of about 1 liter/h by a gas distribution system.
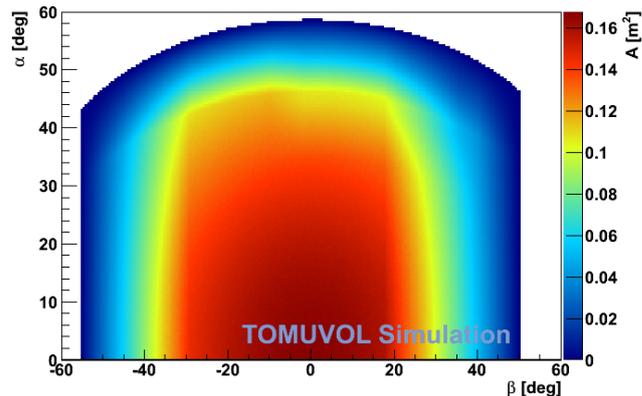
For the data readout, Field Programmable Gate Arrays (FP-GAs) implemented on the detection slabs are connected via their USB interface to a desktop PC. Three independent comparators in the readout electronics provide amplitude information. In the data-taking mode the ASICs buffer every signal above threshold and send the recorded data upon arrival of a trigger signal generated at 10 Hz to the PC on which data acquisition and monitoring software are running. Run control and monitoring software have been customized for the experiment based on the cross-platform acquisition framework XDAQ. The whole setup is controlled remotely through a long-range WIFI network. This link is also used to stream the recorded data to a central server. A video camera surveys the installation at all hours.

To protect the electronics against moisture, the detector has been installed under a tent of polyethylene foil. Additionally, a dehumidifier ventilates dry air under the tent. Environmental data (i.e. temperature, pressure and humidity) are recorded every 15 min and are archived in a data base.

From January to April 2011 data have been taken continuously with two 1 m^2 chambers supplemented by a third chamber of $1/6$ m^2 size. The distance between the first and the second chamber was 49 cm, the one between the second and the third, smaller chamber, 9 cm. The geometrical acceptance of this setup, evaluated with a ray-tracing simulation, is shown as function of the altitude α and the azimuth β (measured w.r.t. the direction of the summit) in Fig. 2. During 65.8 days of data taking with the detector pointing towards the Puy de Dôme, 8 million muon tracks from the entire sky have been recorded. (See Fig. 3) The duty cycle in this phase reached almost 90 percent with only a few short interruptions for detector maintenance operations and systematic tests. After April 6th, the detector support framework was upgraded and a third 1 m^2 chamber replaced the small chamber. A framework for a mobile 1 m^2 detector is now under development. In the following, we will focus on the data obtained with the initial detection setup.
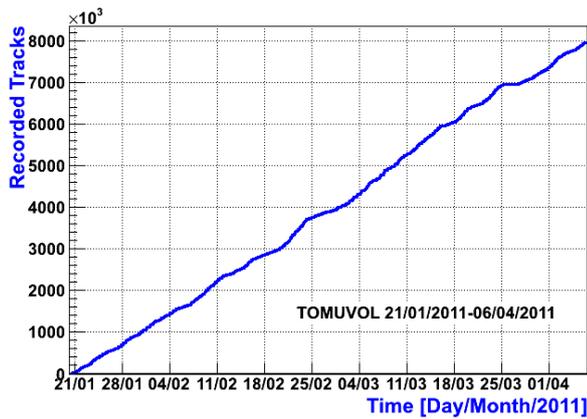
Figure 3: Number of recorded tracks as function of the observation time during the first data-taking phase.

Figure 4: Alignment of the z-position of the second detection plane. The sum of the track χ^2 follows a parabola.

Track Reconstruction The reconstruction algorithm preselects track candidates by considering straight lines between all possible hit combinations in the outermost detection planes in a common time window of $0.4~\mu$s. These track candidates are then filtered by requiring a matching hit in the central detection plane within a distance of 3 cm to the track candidate. For each selected candidate, hits in a corridor of 3 cm are attributed to the track and merged into hit clusters on each detection plane. The final track is then obtained analytically using the method of least squares. After removal of the selected hits from the time frame, the procedure is iterated to identify and reconstruct possible bundles of charged tracks passing the detector simultaneously. The overall quality of the track reconstruction has been verified by inspecting its χ^2-distribution. The χ^2 is defined by the sum of residuals squared divided by the spatial resolution on a 1 cm^2 cell. Its distribution agrees well with the expected exponential form for a straight line fit on three detection planes with two degrees of freedom. Overall, a position resolution of 0.4 cm and an angular resolution of 0.5 deg in both α and β are achieved.

Terrain Survey and Detector Positioning Accurate topographical data are required to compute density images. In March 2011 the Puy de Dôme and its surroundings were mapped precisely with an airborne LIDAR. In this operation the travel time of the emitted laser beam reflected at the ground has been measured and the altitude was calculated with respect to a GPS antenna aboard the aircraft. Analysis of the recorded data is currently underway and an overall precision of better than 10 cm on a 0.5 m grid is expected to be achieved for the final digital elevation model.

To exploit the potentially available precision, the muon detector has been carefully aligned with respect to the volcano. For this purpose GPS based position measurements of the local surroundings have been made. A reference frame in the basement has been defined by tachymetric measurements through the skylights of the basement. Finally the detection planes were positioned with respect to
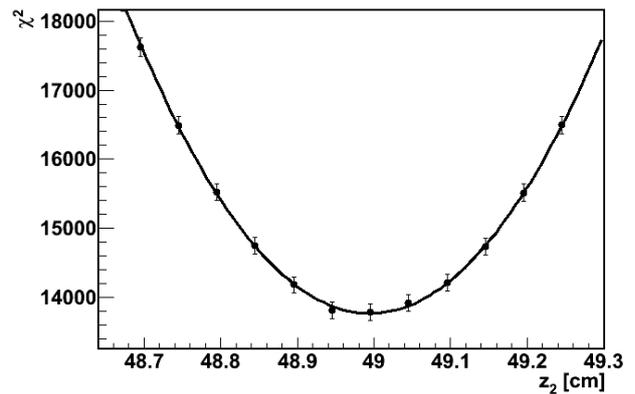
this frame. Additionally, the alignment of the detection planes has been checked with the help of recorded muon tracks. To this end, the sum of the individual track χ^2s is minimized by varying the alignment parameters. An example of this procedure is given in Fig. 4, where the χ^2 is shown as function of the z-coordinate of the second detection chamber together with a parabolic fit. Even if the procedure is limited as the track χ^2 stays invariant under global rescaling of the coordinate axes, it nevertheless provides an important crosscheck of the detector alignment.

3 First Results

Shadow of the Puy de Dôme With the help of the alignment constants obtained as described above, the arrival directions of the recorded muon tracks are transformed into a global coordinate system whose y-axis ($\beta = 0°$) is pointing towards the summit of the volcano. Figure 5 presents the shadow cast in the flux of atmospheric muons by the Puy de Dôme in this coordinate system. For the flux measurement the measured event rates have been divided by the detector acceptance shown in Fig. 2. This preliminary measurement is based on 65.8 days of data taking with an effective
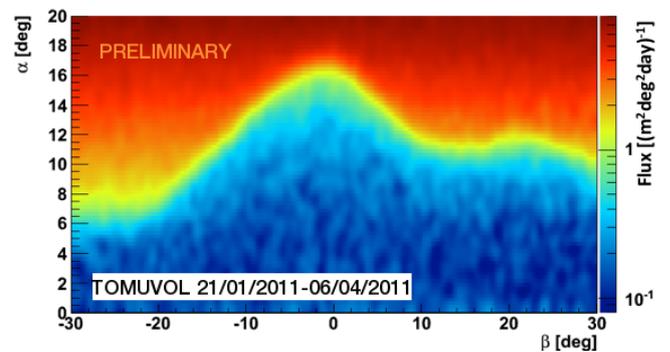
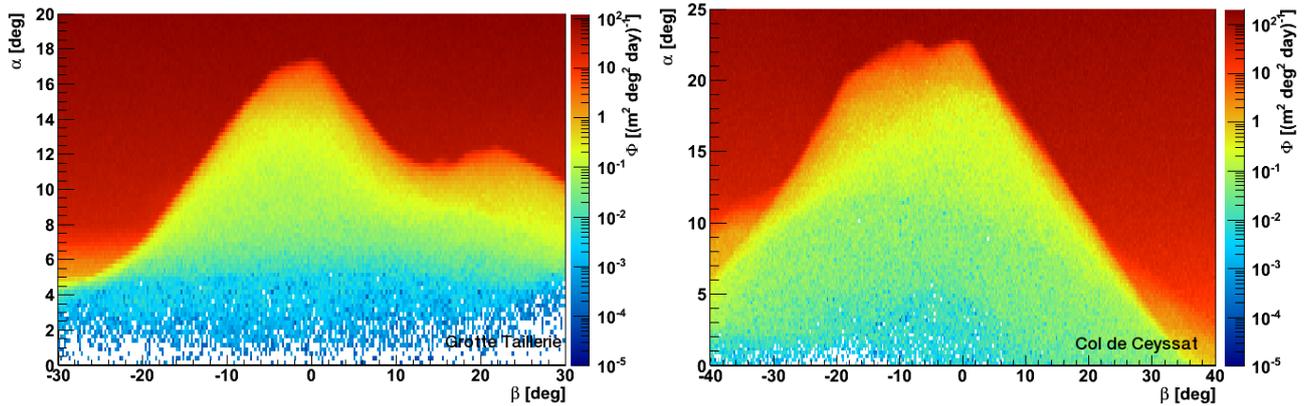Figure 5: Shadow cast in the atmospheric muon flux by the Puy de Dôme.

Figure 6: Estimated muon flux through the "Puy de Dôme" assuming an homogeneous rock density of 1.66 g/cm^3 for two different detection sites located at the flank of the volcano. The simulation confirms that the upper part (red, yellow and green regions in the above plots) of the Puy de Dôme will be accessible for muon imaging with an 1 m^2 detector.

detection area of $\mathcal{A} = 0.16$ m^2. Note that a smoothing algorithm has been applied to the recorded map in order to reduce artificial bands (Moiré-patterns) typical of digital images. Due to the short exposure time of the data set, the significance of the flux through the volcano is statistically limited to regions close to the surface. The observed shape is in good agreement with the actual outline of the volcano. The full statistics accumulated until July 2011 is currently being analyzed in order to extract the first radiographic density distributions.

Expected Muon Fluxes and Prospects of Muon Imaging
Detailed measurements of the nearly horizontal muon flux as function of the muon energy have been carried out by several experiments (e.g. [8]), so that the atmospheric muon flux spectrum can be considered sufficiently well known. Although systematic effects such as altitude dependence and seasonal variations, which, however, mainly affect the low-energy part of the spectrum, might have to be considered in practice. Thus, by propagating muons according to their physical spectrum through the known topography with dedicated propagation codes (e.g. [9]), reliable estimates of the residual muon flux can be derived.

The resulting estimates of the residual muon flux through the Puy de Dôme at two different detection sites at the flank of the volcano are shown in Fig. 6. Note that those distributions are based on an homogeneous rock density of 1.66 g/cm^3 corresponding to preliminary density measurements on the volcano. As a result, the simulation confirms that the Puy de Dôme will be accessible for muon imaging with an 1 m^2 detector.

Besides flux estimates, the simulation also provides a means to measure density distributions. Indeed, only detailed knowledge of absorption curves as function of the traversed depth derived from the simulation gives access to density distributions. Different approaches to compute the density and the corresponding systematic errors are currently studied and will be subject of subsequent publications.

4 Conclusions and Outlook

The TOMUVOL Collaboration explores tomographic imaging of volcanos with atmospheric muons. For this purpose, a GRPC based detector was installed at the flank of the Puy de Dôme in January 2011. Preparatory work for the computation of a tomographic density map, including a precise topographical LIDAR survey of the volcano, have been performed, and the detector has been carefully positioned w.r.t. the volcano. Algorithms for track reconstruction, detector alignment and image reconstruction have been developed and are now applied to first data.

The detector is now going to be relocated to several more places around the volcano in order to realize a complete, three-dimensional density map. In parallel, comparisons with gravimetric and electrical tomographies will be made. Moreover, technical improvements are on the way to enhance the mobility of the detection setup; this should also facilitate future applications to possibly active volcanos under even more challenging environmental conditions.

From the first recorded data and the performed simulation, we can conclude that muon imaging proves to be a promising technique with interesting applications in the near future.

References

[1] E.P. George, Commonwealth Engineer (July 1955), 455

[2] L.W. Alvarez et al., Science 167, (1970), 832

[3] K. Nagamine et al., Proc. Jpn. Acad., Ser B 80 (2004), 179

[4] P. Boivin et al., Volcanologie de la Chaîne des Puys, 5th ed. (2009)

[5] D. Miallier et al., C.R. Geoscience 342 (2010), 847-854

[6] I. Laktineh, Journal of Physics, Conf. Ser 160 (2009), 012030

[7] N. Seguin-Moreau, Proc. of TWEPP Prague (2007) and IEEE Hawei (2007)

[8] S. Matsuno et al., Phys. Rev. D 29 No. 1, (1984)

[9] D. Chirkin, W. Rhode, arXiv:hep-ph/0407075v2